Journal of Applied Pharmaceutical Research
Volume 14 Issue 4, Year of Publication 2026, Page 267 – 276
DOI: https://doi.org/10.69857/joapr.v14i4.2153

Check for updates

Research Article

JOURNAL OF APPLIED PHARMACEUTICAL RESEARCH | JOAPR
www.japtronline.com ***ISSN: 2348 – 0335***

FORMULATION, OPTIMIZATION AND CHARACTERIZATION OF APREMILAST-LOADED NANOSPONGES FOR POTENTIAL TOPICAL WOUND MANAGEMENT APPLICATIONS

Purnima Rai*, Ajay Kumar Singh Rawat

Article Information
Received: 17th March 2026
Revised: 3rd June 2026
Accepted: 5th July 2026
Published: 31st July 2026

Keywords
Apremilast, Nanosponges, Wound management, Topical delivery, Sustained drug release, Entrapment efficiency

ABSTRACT

Background: Topical drug delivery systems provide site-specific therapy with reduced systemic exposure. Nanosponges have emerged as promising carriers owing to their porous structure, enabling improved drug stability, bioavailability, and sustained release. Apremilast, a phosphodiesterase-4 (PDE4) inhibitor with anti-inflammatory activity, has potential for topical wound management when formulated as a controlled-release delivery system. **Methods:** Apremilast-loaded nanosponges were prepared by the emulsion solvent diffusion method using Ethyl Cellulose (EC) and Polyvinyl Alcohol (PVA). A 3^2 factorial design was used to optimize the EC: PVA ratio and sonication time. Formulations were evaluated for particle size, entrapment efficiency, zeta potential, in vitro drug release, and surface morphology. Characterization included UV spectroscopy, FTIR, XRD, DSC, and SEM. Drug release kinetics were analyzed using mathematical models. **Results:** Preformulation studies confirmed drug purity and compatibility with excipients. The optimized formulation (NS8) exhibited a particle size of 213.85 nm, an entrapment efficiency of 82.75%, a zeta potential of −33.3 mV, and a sustained drug release of 95.85% over 24 h. SEM revealed spherical porous nanosponges, while FTIR, XRD, and DSC confirmed drug integrity and formulation stability. Response surface analysis demonstrated significant effects of formulation variables on performance. Drug release followed the Higuchi model ($R^2 = 0.987$), and the Korsmeyer–Peppas exponent (n = 0.58) indicated anomalous non-Fickian diffusion. **Conclusion:** Apremilast-loaded nanosponges demonstrated sustained drug release, excellent stability, and favorable physicochemical characteristics, indicating their potential as an effective topical delivery system for wound management. Further ex vivo, in vivo, and clinical studies are required to confirm therapeutic efficacy and safety.

INTRODUCTION

Wound healing is a complex biological process involving inflammation, proliferation, and tissue remodeling. Wound healing must occur properly, which can be a significant challenge and burden for healthcare systems. Medicare estimated that the cost of treating both acute and chronic wounds

*Maharishi School of Pharmaceutical Sciences, Maharishi University of Information Technology, Lucknow, Uttar Pradesh, 226013, India.

For Correspondence:** **purnima93rai@gmail.com

will be between $28.1 billion and $96.8 billion in 2014 [1,2]. Wound healing is a set of consecutive occurrences. Initially, bleeding and clotting ensue, followed by the activation of an acute inflammatory response to repair the original injury [3]. Extracellular matrix proteins are then generated & the new parenchyma & connective tissue are remodeled. In this process, both connective tissues undergo remodeling, migration, and regeneration. This process involves remodeling, migration, regeneration, and proliferation. Both connective tissue and parenchymal cells proliferate, migrate, and regenerate during this process [4,5].

Collagen deposition is another crucial element. Lastly, parenchymal cells and collagen deposition are crucial elements. Ultimately, these coordinated stages lead to the healing of damaged tissues, which fortifies a wound in a systematic way [6].

Topical drug delivery is the technique of applying a medication-containing formulation directly to the skin to treat a wide range of cutaneous problems, including acne. It can be both therapeutic and patient-friendly [7]. Targeted drug distribution to specific skin patches affected by localized ailments has proven effective. The skin is the primary organ for delivering topical drugs because it is the most accessible site for treating localized ailments [8,9]. Topical drug application is common to prevent several illnesses or ailments. These products include semi-solid formulations utilized in topical drug delivery systems, such as ointments, creams, powders, sprays, gels, and medicated adhesive systems [10].

Materials that resemble sponges and have tiny holes with an average diameter of less than 1μm are called nano-sponges [11]. A sponge can be a long polyester strip dissolved in a fluid containing crosslinkers, which act as microscopic hooking snares to hold various polymer components together. A nanosponge is similar to three-dimensional structures [12].

These tiny sponges may circulate throughout the body until they reach a specific location, adhere to the skin, and, in some cases, begin releasing medication. Because the drug is released at a specific target site rather than circulating throughout the body, it is more effective at a given dose. Within their network, NS may bind less-soluble medications, thereby increasing their bioavailability. They are also very good at entrapping a wide range of excipients [13].

The FDA has authorized a novel drug, apremilast, which inhibits phosphodiesterase 4 enzymes and increases cAMP levels [14]. Tumor necrosis factor alpha (TNF) production by human rheumatoid synovial cells is spontaneously suppressed as a result of phosphodiesterase-4 inhibition. The development of Apremilast-loaded nanosponges may improve drug stability, sustain drug release, and potentially enhance topical delivery characteristics [15]. Topical amphotericin B nanosponge gel penetrates the skin and helps deliver a higher therapeutic dose through the epidermis [16].

The advantages of utilizing experimental design to optimize nanoparticles include fewer experiments, the construction of mathematical models to estimate the statistical significance &importance of factor effects, and the assessment of component interaction effects [17]. A two-factor, three-level experimental strategy was used to optimize the NS synthesis procedure.

MATERIAL AND METHODS

Materials

The materials listed below were obtained from the specified sources without further purification. Apremilast was obtained from INSCHEM, which is based in Lucknow, Uttar Pradesh, India. The remaining chemicals utilized were analytical reagent grade.

Methods

Pre-formulation research

Pre-formulation studies of apremilast included physicochemical and compatibility characterization [18]. The melting point was determined using the capillary method in a liquid paraffin bath, and the temperature at complete melting was recorded [19]. Solubility was evaluated by the shake-flask method in water, ethanol, isopropyl myristate, and octanol. For UV–visible spectroscopic analysis, a standard stock solution (100 μg/mL) was prepared in ethanol and diluted to 1–6 μg/mL; spectral scanning was performed over 200–400 nm to determine the absorption maximum. Fourier Transform Infrared (FT-IR) spectroscopy was conducted using the KBr pellet method to identify characteristic functional groups and confirm structural integrity [20,21]. Drug–excipient compatibility was assessed by storing a 1:1 physical mixture in hermetically sealed vials at ambient conditions for four weeks, followed by FT-IR analysis [22]. X-ray diffraction (XRD) was performed to evaluate crystallinity and diffraction patterns of the pure drug [23]. Differential scanning calorimetry (DSC) analysis was carried

out using sealed aluminum pans, heated from 50–300 °C at 5 °C/min under nitrogen purge (30 mL/min), with an empty pan as reference [24,25].

Formulation Development

Preparation of Nano-emulsion as per the Experimental Design

A two-factor, three-level experimental design using Design-Expert® (v12.0.3.0) was employed to optimize the nanosponge formulation with only nine experimental runs, reducing time and resource consumption [26,27]. The independent variables were the relative concentration ratio of Ethyl Cellulose (EC) in the organic phase to Polyvinyl Alcohol (PVA) in the aqueous phase (X1) and sonication time (X2). The EC: PVA factor represents the polymer-to-stabilizer concentration ratio (w/v) employed during emulsification [28].

Table 1: Variables in 3^2 factorial design

Factor Independent variables	Levels used		
	-1	0	+1
Concentration of EC: PVA Ratio (%) (X1)	1	3	5
Sonication Time (X2)	10	15	20
Dependent variables	**Constraints**		
Particle size (nm) (Y1)	Minimize		
% Entrapment Efficiency (%) (Y2)	Maximize		
% Drug Release (%) (Y3)	Maximize		

Table 2: Composition and observed responses in 3^2 factorial design

Batch	Drug (mg)	Independent Factors		Dependent Factors		
		Concentration of EC: PVA ratio (%)	Sonication Time (Min)	Particle size (nm)	% EE	%DR
NS1	20	5.82843	15	197.13	63.24	76.83
NS2	20	1	10	202.6	60.22	79.81
NS3	20	5	20	207.5	69.82	74.94
NS4	20	1	20	229.21	60.23	91.93
NS5	20	3	7.92893	216.13	70.91	93.41
NS6	20	0.171573	15	211.34	61.95	82.56
NS7	20	3	22.0711	237.42	73.22	81.56
NS8	20	3	15	213.85	82.75	95.85
NS9	20	5	10	208.57	65.82	88.71

Formulation by Emulsion Solvent Diffusion Method

Apremilast-loaded nanosponges were prepared using the emulsion solvent diffusion method. Ethyl Cellulose (EC) was incorporated into the organic phase, while Polyvinyl Alcohol (PVA) was dissolved in the external aqueous phase. The experimental factor designated as EC: PVA ratio refers to the relative concentrations of EC and PVA in their respective phases during emulsification. Apremilast was completely dissolved using magnetic stirring. This organic phase was added dropwise into an aqueous external phase containing polyvinyl alcohol (PVA) dissolved in 100 mL of distilled water**,** under continuous stirring at 800–1000 rpm for 2 hours. The resulting nanosponge dispersion was filtered and dried at 40°C for 24 hours**.** The dried powder was collected and used for further characterization studies.

EVALUATION OF NANOSPONGE

Percentage encapsulation efficiency

When evaluating the efficacy of a medication delivery strategy, encapsulation efficiency is a crucial factor. This technique entails forming a shell around a medicine to keep it from leaching out before reaching its target. Encapsulation efficiency is the percentage of the drug that is successfully trapped within the nano-sponges, indicating how much medicine is efficiently supplied in comparison to how much is encapsulated. The drug was loaded. Nano-sponges were centrifuged at 13000 rpm for 40 minutes, and the supernatant was analyzed for unbound drug using a UV spectrophotometer at 230 nm. The percentage encapsulation efficiency was then calculated.

In vitro Drug release

In vitro drug release of nanosponge (NS8) formulations was performed using a diffusion assembly similar to a Franz diffusion cell. A pre-soaked cellophane membrane was tightly secured over the open end of a glass tube using a rubber band to ensure water tightness, forming the donor compartment. Accurately weighed NS (100 mg) was placed in the donor chamber. The receptor compartment consisted of 50 mL phosphate-buffered saline (PBS, pH 7.1) in a 100 mL beaker, thermostatically maintained at 37 °C and stirred at 50 rpm. The donor tube was positioned vertically into the receptor medium. At predetermined intervals up to 24 h, 5mL samples were withdrawn and replaced with fresh medium to maintain sink conditions. Drug concentration was determined spectrophotometrically at 230 nm.

Release Kinetics

The pharmacokinetic principle indicates that the drug release kinetics for dosage forms can be described by multiple equations corresponding to different kinetic models.

Particle Morphology

Scanning electron microscopy (SEM) is used to examine nanosponges' surface morphology.

RESULT AND DISCUSSION

Pre-formulation studies confirmed apremilast purity. DSC analysis showed a sharp endothermic melting peak at 157.25–159.56°C, consistent with the crystalline nature of Apremilast. FTIR and DSC showed no drug-excipient incompatibility, while XRD further confirmed crystallinity.

Solubility Study

Solubility testing of Apremilast was carried out in various solvents including dichloromethane (DCM), ethanol, methanol, chloroform, acetone, octanol & water. Apremilast was found to be soluble in all tested organic solvents, including DCM, while it was insoluble in water. The results are presented in Table 3. The high solubility of Apremilast in DCM supported its selection as the organic phase solvent during nanosponge preparation.

Table 3: Solubility test for Apremilast in different solvents

Sr. No.	Solvent	Soluble Status
1	Ethanol	Soluble
2	Methanol	Freely Soluble
3	Chloroform	Soluble
4	Acetone	Soluble
5	Dichloromethane (DCM)	Soluble
6	Octanol	Slightly Soluble
7	Water	Insoluble

UV-visible Spectroscopy

The absorption maximum (λmax) of apremilast was determined in ethanol. It was found to be 230 nm, as shown in Figure 1. The UV–Vis spectrum shows a strong absorption peak at ~230 nm, indicating key electronic transitions & enabling both qualitative identification & quantitative analysis of the compound.

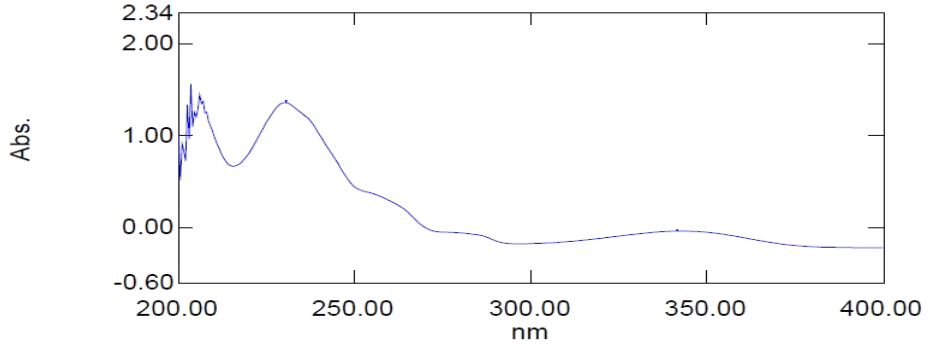

Figure 1: UV Spectrum of Apremilast

Fourier Transform Infra-Red Spectroscopy (FTIR)

FTIR spectrum of Apremilast showed characteristic peaks at 1764.75 and 1705.14 cm^{-1} (C=O stretching), 3003.02 cm^{-1} (aromatic C–H stretching), and 1618.23 cm^{-1} (C=C stretching), confirming the presence of key functional groups. These results validate the structural integrity and purity of Apremilast by matching with reference spectral data. The FTIR spectrum is shown in Figure 2.

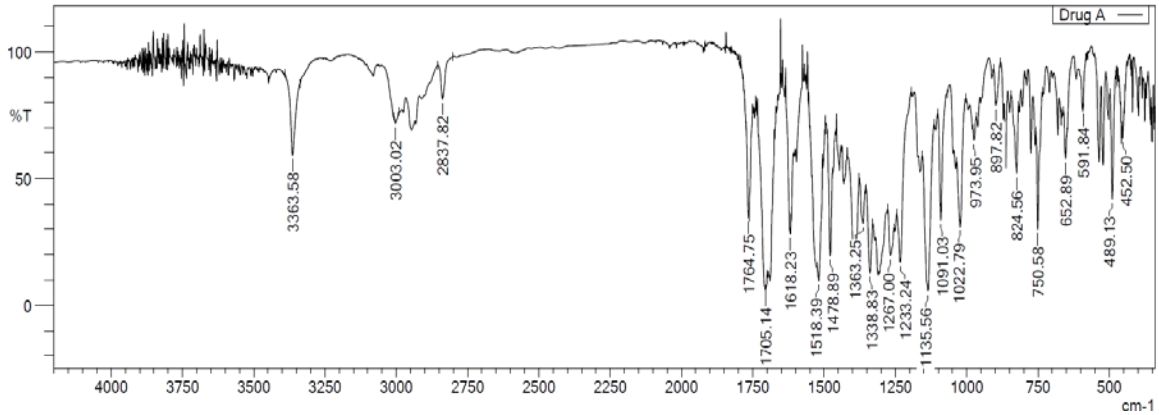

Figure 2: FTIR Spectrum of Apremilast

Drug-excipient compatibility studies

FTIR spectra showed characteristic peaks of Apremilast and excipients, including O–H/N–H (4333.95, 3364.30 cm^{-1}), C–H (2888.82 cm^{-1}), C=O (1763.31 cm^{-1}), and C–O (1262.05, 1234.67 cm^{-1})**,** confirming the presence of functional groups from the drug and polymers.No significant peak shift or disappearance was observed, indicatingdrug–excipient compatibility and successful incorporation with maintained formulation stability, shown in figure 3.

X-ray diffraction (XRD) study

XRD analysis of Apremilast showed sharp diffraction peaks at 10°, 15°, 20°, and 25°**,** with a prominent peak at 20°, confirming its highly crystalline and well-ordered lattice structure.The close agreement with theoretical data indicates phase purity, absence of polymorphism, and suitability for pharmaceutical application**,** as shown in Figure 4.

Differential Scanning Calorimetry (DSC)

The DSC thermogram of Apremilast shows a sharp endothermic peak at 157.25–159.56°C corresponding to its melting point, confirming its crystalline nature and purity, with no significant thermal transitions before melting and decomposition occurring at higher temperatures (300–400°C), as shown in Figure 5.

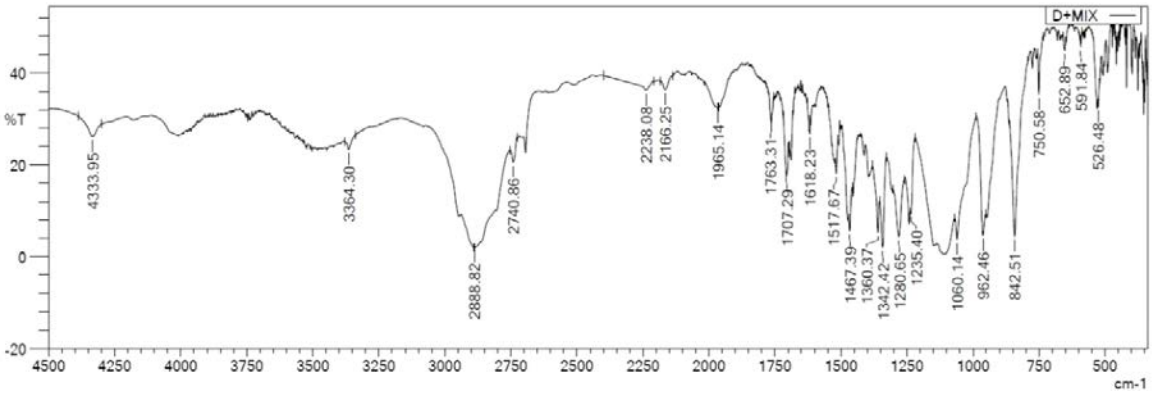

Figure 3: FTIR spectrum of drug with excipients

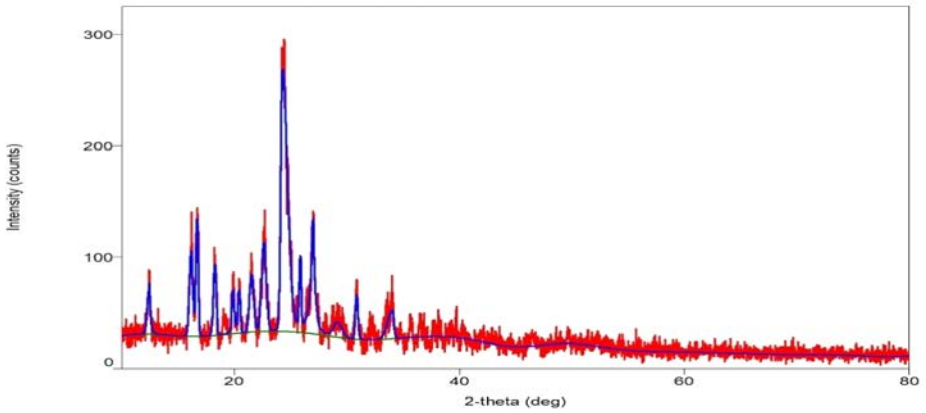

Figure 4: XRD of Apremilast

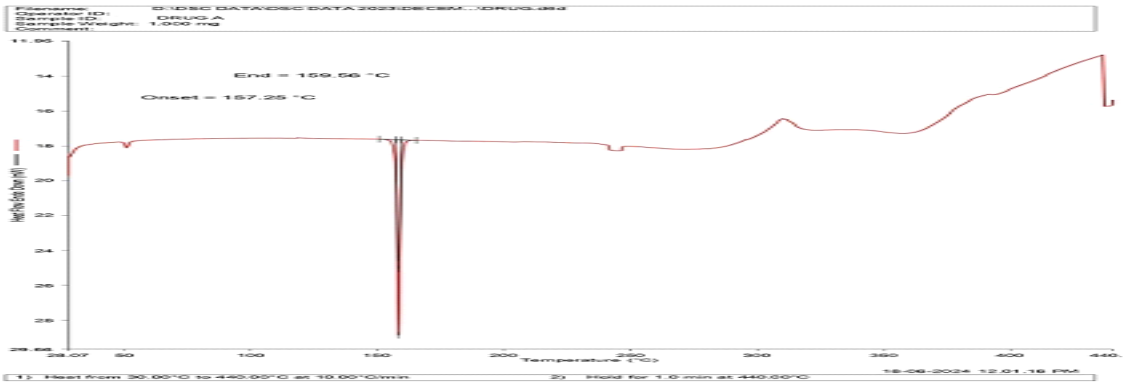

Figure 5: DSC of Apremilast

Formulation Development

Experimental Design for the Formulation of Nanosponges

3^2 factorial design optimized nanoparticle formulation by evaluating the effects and interactions of process variables, with the quadratic model showing the best fit for both dependent responses across 9 experimental runs, confirming the statistical significance and reliability of the optimization process. The adequacy of the quadratic response surface models was confirmed by ANOVA analysis. The developed models exhibited statistically significant F-values ($p < 0.05$), satisfactory coefficients of determination (R^2), and non-significant lack-of-fit values, indicating good agreement between the experimental and predicted responses.

Effect of independent variables on particle size

Figure 6 presents the 3D response surface plot illustrating the influence of formulation variables on nanosponge particle size, a critical determinant of drug release kinetics and absorption. Particle size decreased with increasing EC: PVA ratio, indicating that higher polymer–stabilizer ratios promote formation of smaller nanoparticles. Sonication time exhibited a nonlinear effect: particle size initially declined with increasing time; at extended durations, particle size stabilized or increased slightly. Optimal size reduction was achieved at moderate sonication times combined with higher EC: PVA ratios. Excessive sonication or low EC: PVA ratios led to particle enlargement, likely due to coalescence or inadequate polymer dispersion.

$$\textit{Particle Size} = 205.9644 + 16.6771(X_1) - 3.2272(X_2) - 0.6920(X_1)(X_2) - 1.4228(X_1)^2 + 0.22315(X_2)^2 \quad (1)$$

Effect of independent variables on % Entrapment efficiency:

The 3-D response surface analysis, as shown in Figure 7, demonstrates that entrapment efficiency (%EE) is significantly influenced by both EC: PVA ratio and sonication time. %EE increased from 59.62% to 82.25% with higher EC: PVA ratios due to greater polymer availability for drug encapsulation. Prolonged sonication (10–20 minutes) reduced %EE, likely due to nanoparticle disruption or drug leakage. A higher EC: PVA ratio with shorter sonication achieved optimal entrapment efficiency.

$$\%\, EE = 107.1874 + 2.7687(X_1) - 7.7086(X_2) - 0.2250(X_1)(X_2) + 0.1429(X_1)^2 + 0.3075(X_2)^2 \quad (2)$$

Effect of independent variables on % Drug Release

Figure 8 presents the 3D response surface plot illustrating the effect of formulation variables on percentage drug release, demonstrating significant modulation of in vitro release behavior.

$$\%\, \textit{In vitro drug release} = 21.5705 + 20.7163(X_1) + 6.4232(X_2) - 0.6472(X_1)(X_2) - 2.0032(X_1)^2 - 0.1647(X_2)^2 \quad (3)$$

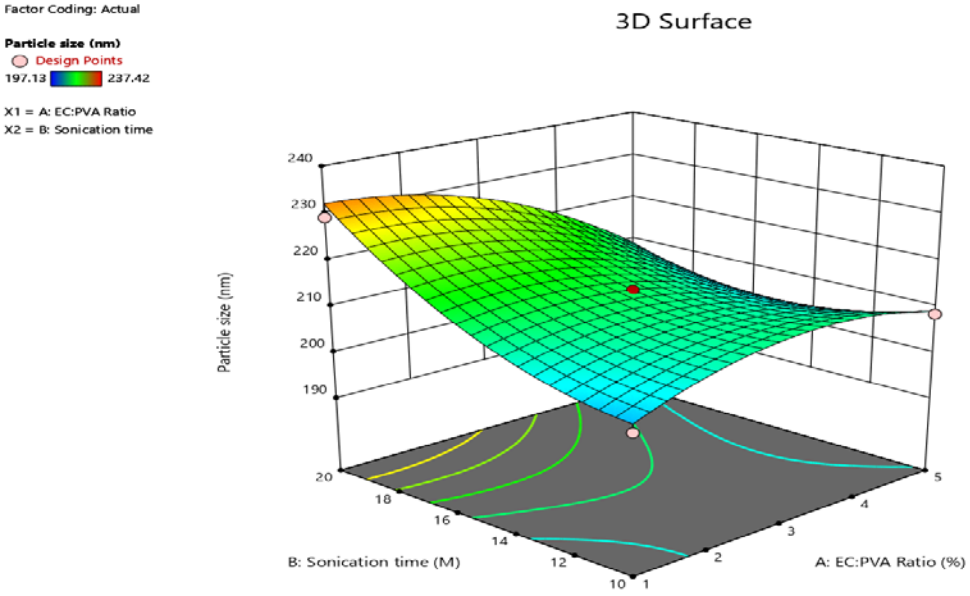

Figure 6: Response 3D plots for the effect of EC: PVA ratio (X1) and sonication time (X2) on particle size

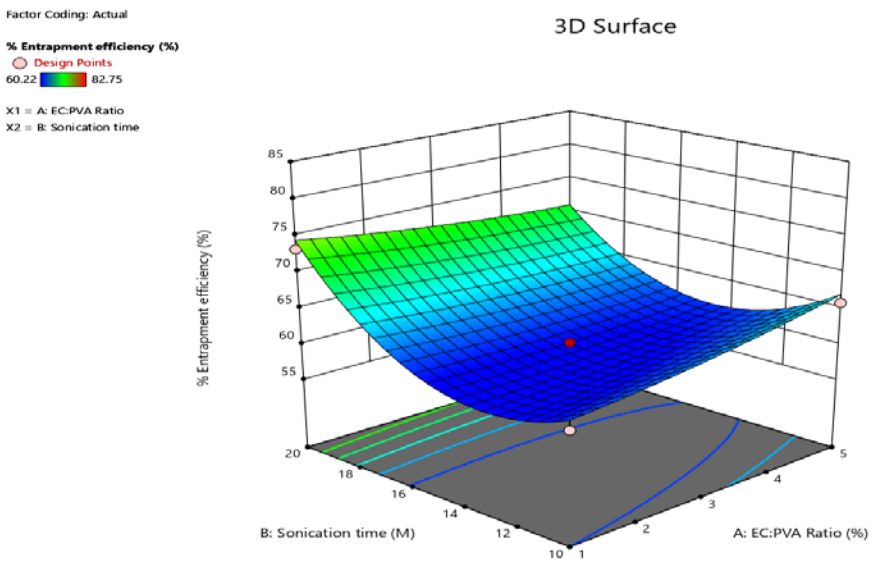

Figure 7: Response 3D plots for the effect of EC: PVA ratio (X1) and sonication time (X2) on % Entrapment efficiency

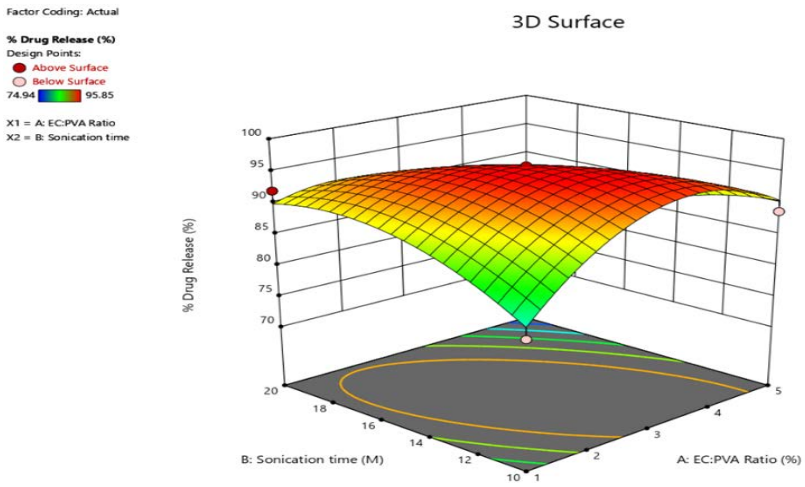

Figure 8: Response 3D plots for the effect of EC: PVA ratio (X1) and sonication time (X2) on % drug release.

The study demonstrates that increasing the EC: PVA ratio reduces drug release (90–95% to 75–85%) due to formation of a denser polymeric matrix, while optimal sonication time (12–14 minutes) maximizes release efficiency, confirming that formulation and processing parameters critically regulate nanosponges' drug release kinetics.

From a physiological perspective, the sustained release profile of the optimized Apremilast-loaded nanosponges is particularly relevant to the early stages of wound healing. Following tissue injury, the acute inflammatory phase begins immediately. It typically predominates during the first 24–72 hours, characterized by neutrophil recruitment, macrophage activation, and elevated production of pro-inflammatory mediators such as TNF-α, IL-17, and other cytokines. As Apremilast acts through phosphodiesterase-4 (PDE4) inhibition to modulate inflammatory signaling pathways, the observed sustained drug release of 95.85% over 24 hours may help maintain therapeutic drug levels at the wound site throughout the critical initial inflammatory period. Continuous local availability of Apremilast during this phase could help control excessive inflammation while supporting the transition toward the proliferative stage of tissue repair. Therefore, the 24-hour release window demonstrated by the optimized nanosponge formulation is physiologically aligned with the temporal requirements of early wound healing. However, this proposed benefit remains hypothetical and requires confirmation through appropriate in vivo wound-healing studies.

Although the optimized nanosponge formulation demonstrated favorable physicochemical characteristics and sustained drug release behavior, no ex vivo skin permeation or biological wound-healing studies were performed in the present investigation. Therefore, the observed formulation advantages should be interpreted as indicators of potential topical performance rather than direct evidence of enhanced wound healing efficacy. The ANOVA summary is presented in Table 4.

Table 4: Combined ANOVA Summary for Response Surface Models

Response	Model F-value	Model p-value	R^2	Adjusted R^2	Model Significance
Particle Size (Y_1)	24.97	0.0119	0.9765	0.9374	Significant
Entrapment Efficiency (Y_2)	21.47	0.0148	0.9728	0.9275	Significant
Drug Release (Y_3)	9.09	0.0494	0.9381	0.8349	Significant

The optimized nanosponge formulation showed:

- Particle size: **213.85 nm**
- Entrapment efficiency: **82.75%**
- Drug release (24 h): **95.85%**
- Zeta potential:**−33.3 mV**

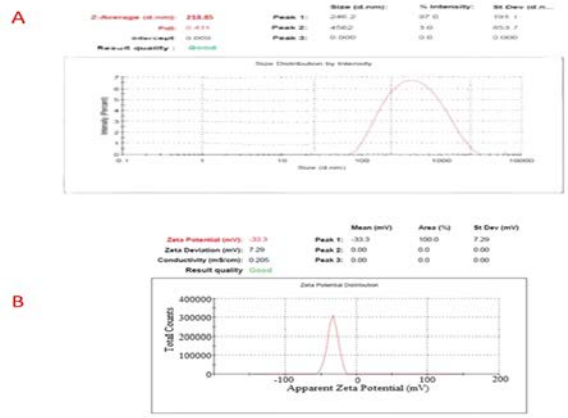

Figure 9: A. Particle size distribution B. Zeta Potential of optimized batch nanosponges

Particle Morphology

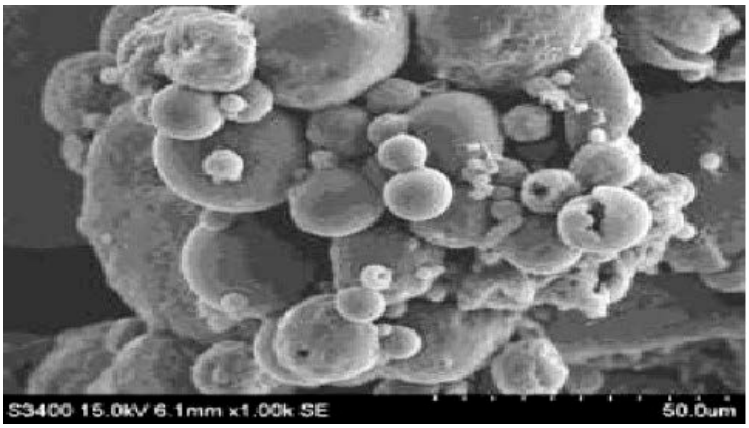

Figure 10: SEM image of Optimized batch of Apremilast Nanosponges

SEM, as shown in Figure 10, revealed spherical porous nanosponges that may support controlled drug-release behavior.

EVALUATION OF NANO-SPONGES

Percentage encapsulation efficiency

The %EE of prepared apremilast nanosponges (NS1-NS9) ranged from 60.22 to 82.75% (Table 2). Based on the results, apremilast nanosponges (NS8) were optimized with % EE (82.75%).

In-vitro drug release

The in vitro drug release of prepared apremilast nanosponges (NS1–NS9) was found to be in the range of 74.94 – 95.85 % (Table 2). Based on the results, apremilast nanosponges (NS8) were optimized for in vitro drug release (95.85 %).

Drug Release Kinetics

To investigate the release mechanism of Apremilast from the optimized nanosponge formulation (NS8), in vitro drug release data were evaluated using various kinetic models: Zero-order, First-order, Higuchi, and Korsmeyer–Peppas. The results, summarized in Table 5, indicated that the Higuchi model had the highest correlation coefficient (R^2 = 0.987), suggesting that the drug release primarily occurred via diffusion from the polymeric matrix. The Korsmeyer–Peppas model also demonstrated a strong fit (R^2 = 0.981), confirming diffusion-controlled release. The release exponent (n) from the Korsmeyer–Peppas equation was determined to be 0.58, indicating anomalous (non-Fickian) transport, which involves both diffusion and polymer relaxation mechanisms. This n value supports the conclusion that Apremilast release from the nanosponge matrix follows a non-Fickian diffusion mechanism. Overall, these findings quantitatively affirm the sustained-release behavior of the optimized formulation observed over 24 hours, illustrating the efficacy of the porous ethyl cellulose nanosponge matrix in controlling drug release through diffusion-assisted transport.

Table 5: Drug Release Kinetic Modeling of Optimized Apremilast Nanosponge Formulation (NS8)

Model	Equation	R^2
Zero Order	Qt = Q0 + K0t	0.942
First Order	Log Qt	0.918
Higuchi	$Q = KH\sqrt{t}$	0.987
Korsmeyer-Peppas	$Mt/M\infty = Ktn$	0.981

Particle size distribution & polydispersity index

The average particle size of Apremilast nanosponges was 213.85 nm, according to the particle size analysis, and their polydispersity index (PDI) value was 0.411.

Zeta potential

Zeta potential analysis showed a surface charge of −33.3 mV (Figure 9), indicating good electrostatic stability and favorable interaction potential with biological systems.

CONCLUSION

The present study successfully developed and optimized Apremilast-loaded nanosponges using the emulsion solvent diffusion method in combination with a 3^2 factorial design. The formulation variables, namely EC: PVA ratio and sonication time, significantly influenced particle size, entrapment efficiency, and drug release behavior, as confirmed by response surface analysis and ANOVA. The optimized nanosponge formulation (NS8) exhibited a particle size of 213.85 nm, entrapment efficiency of 82.75%, zeta potential of −33.3 mV, and sustained drug release of 95.85% over 24 h, indicating favorable physicochemical stability and controlled-release characteristics. Physicochemical characterization using FTIR, XRD, DSC, and SEM confirmed drug–excipient compatibility, retention of the crystalline nature of Apremilast, and the formation of spherical porous nanosponges. Drug release kinetic analysis demonstrated that the optimized formulation followed the Higuchi model (R^2 = 0.987). In contrast, the Korsmeyer–Peppas release exponent (n = 0.58) indicated anomalous non-Fickian diffusion, suggesting that drug release occurred through a combination of diffusion and polymer relaxation mechanisms. The sustained-release profile observed over 24 h highlights the potential of the nanosponge system to maintain prolonged local drug availability. Overall, the developed Apremilast-loaded nanosponges represent a promising topical drug delivery platform with potential applicability in future wound-healing therapies. However, since the present investigation was limited to physicochemical characterization and in vitro evaluation, further ex vivo skin permeation, in vivo wound-healing, safety, and clinical studies are necessary to establish therapeutic efficacy and translational potential.

FINANCIAL ASSISTANCE

NIL

CONFLICT OF INTEREST

The authors declare no conflict of interest.

AUTHOR CONTRIBUTION

The study was conceptualized and designed by Purnima Rai, who also performed the experimental procedures, gathered and analyzed the data, and drafted the initial version of the manuscript. AKS Rawat provided support in developing the methodology, oversaw the progress of the project, contributed to data interpretation, and thoroughly revised the manuscript for critical intellectual content. All authors have reviewed and approved the final manuscript and take full responsibility for the integrity and accuracy of the work.

DECLARATION OF USE OF AI TOOLS

The authors used ChatGPT to assist with language editing and improving readability. All content, analysis, and conclusions were reviewed and verified by the authors. The authors take full responsibility for the originality, accuracy, and integrity of the work.

REFERENCES

[1] Sen CK. Human wound and its burden: Updated 2022 compendium of estimates. *Adv. Wound Care (New Rochelle).*, **12(12)**, 657–670 (2023) https://doi.org/10.1089/wound.2023.0150

[2] Olsson M, Järbrink K, Divakar U, Bajpai R, Upton Z, Schmidtchen A, et al. The humanistic and economic burden of chronic wounds: A systematic review (update). *Wound Repair Regen.*, **31(1)**, 1–13 (2023) https://doi.org/10.1111/wrr.13077

[3] Wilkinson HN, Hardman MJ. Wound healing: Cellular mechanisms and pathological outcomes. *Open Biol.*, **10(9)**, 200223 (2020) https://doi.org/10.1098/rsob.200223

[4] Eming SA, Murray PJ, Pearce EJ. Metabolic orchestration of the wound healing response. *Cell Metab.*, **33(9)**, 1726–1743 (2021) https://doi.org/10.1016/j.cmet.2021.07.017

[5] Lambi AG, DeSante RJ, Patel PR, Hilliard BA, Popoff SN, Barbe MF. Blocking CCN2 reduces established palmar neuromuscular fibrosis and improves function following repetitive overuse injury. *Int. J. Mol. Sci.*, **24(18)**, 13866 (2023) https://doi.org/10.3390/ijms241813866

[6] Khanam S. A systematic review on wound healing and its promising medicinal plants. *IP Int. J. Compr. Adv. Pharmacol.*, **5(3)**, 170–176 (2021) https://doi.org/10.18231/j.ijcap.2020.030

[7] Benson HAE, Grice JE. Topical drug delivery: Principles and practice. *Adv. Drug Deliv. Rev.*, **186**, 114320 (2022) https://doi.org/10.1016/j.addr.2022.114320

[8] Mohd Saeed, et al. Recent advances in topical drug delivery systems for skin disorders. *Gels*, **9(2)**, 123 (2023) https://doi.org/10.3390/gels9020123

[9] Badran YAA, Kuntsche J, Fahr A. Skin penetration enhancement strategies in topical drug delivery. *Pharmaceutics*, **13(9)**, 1361 (2021) https://doi.org/10.3390/pharmaceutics13091361

[10] Singh A, Verma A, Kumar P. Innovative nanostructured lipid carrier gel for enhanced topical delivery of roflumilast in psoriasis management. *Journal of Applied Pharmaceutical Research*, **13(4)**, 254-265 (2025) https://doi.org/10.69857/joapr.v13i4.1242

[11] Swaminathan S, Vavia PR, Trotta F, Cavalli R. Nanosponges for drug delivery and biomedical applications: Recent progress. *Gels*, **9(3)**, 210 (2023) https://doi.org/10.3390/gels9030210

[12] Shende PK, Gaud RS. Nanosponges: A potential nanocarrier for drug delivery. *J. Drug Deliv. Sci. Technol.*, **53**, 101187 (2019) https://doi.org/10.1016/j.jddst.2019.101187

[13] Krishnamoorthy K, Mahalingam S. Nanosponges: A novel class of drug delivery system—Recent trends and advances. *J. Drug Deliv. Sci. Technol.*, **68**, 103043 (2022) https://doi.org/10.1016/j.jddst.2021.103043

[14] Sakkas LI, Bogdanos DP. Apremilast: A novel PDE4 inhibitor for inflammatory diseases. *Clin. Immunol.*, **226**, 108730 (2021) https://doi.org/10.1016/j.clim.2021.108730

[15] Papp K, Reich K, Paul C, et al. Apremilast in inflammatory dermatologic diseases: Updated clinical evidence. *J. Am. Acad. Dermatol.*, **86(1)**, e1–e14 (2022) https://doi.org/10.1016/j.jaad.2021.05.067

[16] Kaur IP, Aggarwal D, Singh H, Kakkar S. Nanosponges as a promising carrier for topical delivery of antifungal agents: Recent advances. *J. Drug Deliv. Sci. Technol.*, **70**, 103210 (2022) https://doi.org/10.1016/j.jddst.2022.103210

[17] Luiz MT, Viegas JSR, Abriata JP, Viegas F, Vicentini FTMC, Bentley MVLB, et al. Design of experiments (DoE) to develop and optimize nanoparticles as drug delivery systems. *Eur. J. Pharm. Biopharm.*, **165**, 127–148 (2021) https://doi.org/10.1016/j.ejpb.2021.05.011

[18] Tekade RK. Basic fundamentals of pharmaceutical formulation development and preformulation studies. *Pharmaceutics*, **13(10)**, 1684 (2021) https://doi.org/10.3390/pharmaceutics13101684

[19] Rampado R, Peer D. Design of experiments in the optimization of nanoparticle-based drug delivery systems. *J. Control. Release*, **358**, 398–419 (2023) https://doi.org/10.1016/j.jconrel.2023.05.001

[20] Jain S, Shah RP. Drug-excipient compatibility study through a novel vial-in-vial experimental setup: A benchmark study. *AAPS PharmSciTech*, **24(5)**, 117 (2023) https://doi.org/10.1208/s12249-023-02573-0

[21] Tkachenko Y, Niedzielski P. FTIR as a method for qualitative assessment of solid samples in geochemical research: A review. *Molecules*, **27(24)**, 8846 (2022) https://doi.org/10.3390/molecules27248846

[22] Park YS, Choi J, Kim BS, et al. Synergistic effects of P and Si on the flame retardancy in a polymethyl silsesquioxane aerogel prepared under ambient pressure drying. *J. Therm. Anal. Calorim.*, **148**, 7623–7632 (2023) https://doi.org/10.1007/s10973-023-12244-8

[23] Ponsar H, Quodbach J. Customizable 3D printed implants containing triamcinolone acetonide: Development, analysis, modification, and modeling of drug release. *Pharmaceutics*, **15(8)**, 2097 (2023) https://doi.org/10.3390/pharmaceutics15082097

[24] Buya AB, Mahlangu P, Witika BA. From lab to industrial development of lipid nanocarriers using quality by design approach. *Int. J. Pharm. X*, Article 100266 (2024) https://doi.org/10.1016/j.ijpx.2024.100266

[25] Khan I, Saeed K, Khan I. Nanoparticles: Properties, applications and toxicities. *Arab. J. Chem.*, **12(7)**, 908–931 (2019) https://doi.org/10.1016/j.arabjc.2017.05.011